

Supplementary Materials for

Functional diversification of hybridoma-produced antibodies by CRISPR/HDR genomic engineering

Johan M. S. van der Schoot, Felix L. Fennemann, Michael Valente, Yusuf Dolen, Iris M. Hagemans, Anouk M. D. Becker, Camille M. Le Gall, Duco van Dalen, Alper Cevirgel, Jaco A. C. van Bruggen, Melanie Engelfriet, Tomislav Caval, Arthur E. H. Bentlage, Marieke F. Fransen, Maaïke Nederend, Jeanette H. W. Leusen, Albert J. R. Heck, Gestur Vidarsson, Carl G. Figdor, Martijn Verdoes*, Ferenc A. Scheeren*

*Corresponding author. Email: martijn.verdoes@radboudumc.nl (M.Ve.); f.a.scheeren@lumc.nl (F.A.S.)

Published 28 August 2019, *Sci. Adv.* **5**, eaaw1822 (2019)
DOI: 10.1126/sciadv.aaw1822

This PDF file includes:

- Fig. S1. Genomic map and annotated base pair sequence of rIgG2a constant domains.
- Fig. S2. Sortagging of Fab' fragments derived from CRISPR/HDR-engineered hybridomas.
- Fig. S3. Characterization of MIH5 Fc variants hybridomas.
- Fig. S4. Raw images of sortagging of MIH5 isotype variants.
- Fig. S5. Murine isotype panel generation of NLDC-145 via CRISPR/HDR.
- Fig. S6. Glycosylation profile of MIH5 mIgG2a via native mass spectrometry.
- Fig. S7. Gating and FACS plots of isotype-dependent depletion in vivo.
- Table S1. Fab' donor construct for HDR.
- Table S2. Isotype donor constructs for HDR.
- Table S3. FcγR affinity values of MIH5 Fc variants and comparison to literature.

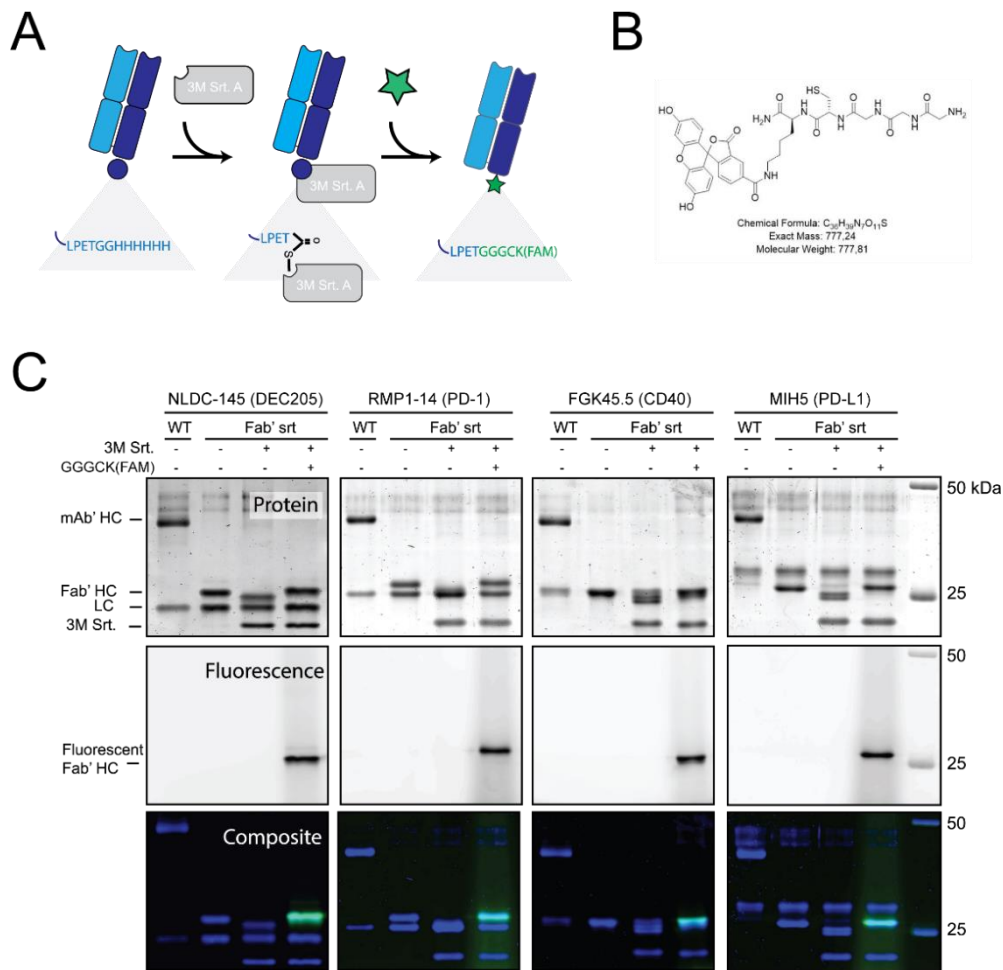


Fig. S2. Sortagging of Fab' fragments derived from CRISPR/HDR-engineered hybridomas. The CRISPR/HDR strategy as outlined in Fig. 1 was also performed on hybridomas RMP1-14 (PD-1), FGK45.5 (CD40) and MIH5 (PD-L1). The resulting Fab' hybridomas all secreted the designed Fab' fragments which could be easily isolated from the supernatant, demonstrating universal applicability of this approach. **(A)** All Fab' fragments were equipped with a c-terminal sortag motif to perform sortase mediated ligation. **(B)** We synthesized the fluorophore GGGCK(FAM) to functionalize the c-terminus of the Fab' fragment heavy chain. **(C)** To this purpose, we incubated 5µg of Fab' fragment (10µM) with equimolar amounts of an evolved sortase (3M Srt., 10µM) and with or without 50 molar equivalents of GGGCK(FAM) for one hour at 37°C. From each reaction mix we loaded 5µg on reducing SDS-page together with the parental mAb and unmodified Fab and acquired the protein and fluorescent scans. The left panel displays the protein and fluorescent scans of Fab'DEC205-srt, of which the composite is shown in Fig. 1G.

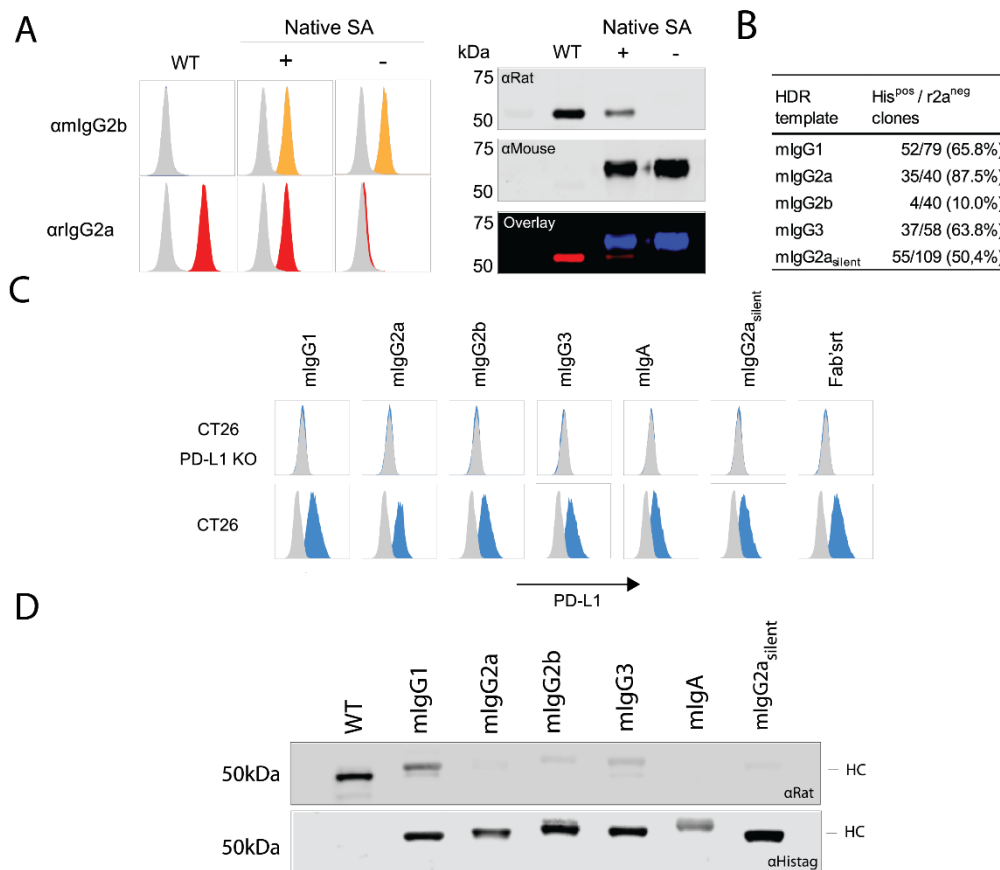


Fig. S3. Characterization of MIH5 Fc variants hybridomas. (A) Presence of the original splice acceptor adjacent to the rat CH1 exon in the donor construct results in background secretion of the native rIgG2a MIH5 in the supernatant. In the supernatant of engineered hybridomas where the splice acceptor is removed, production of the native isotype is abrogated as determined by flow cytometry (left panels) and western blot (right panels). The data shown is from two MIH5 mIgG2b clones, which were generated using donor constructs with (+) or without (-) the native splice acceptor in the 3' homology arm of the donor construct. (B) Table displaying the number of clones after CRISPR/HDR employing HDR templates in which the native splice acceptor has been removed for all murine isotypes, followed by selection, that secrete the designed MIH5 isotype variant (His^{pos}/r2a^{neg}). Clones were analyzed by flow cytometry with secondary antibodies against his-tag and rat IgG2a isotype on CT26 stained with supernatant from monoclonal cell suspensions. (C) Flow cytometry plots of CT26 and CT26^{PD-L1 KO} stained with MIH5 Fc variants in combination with a secondary antibody against his-tag, indicating that specificity for PD-L1 is retained. (D) Western blot analysis demonstrates substitution of the rat heavy chain for murine heavy chains.

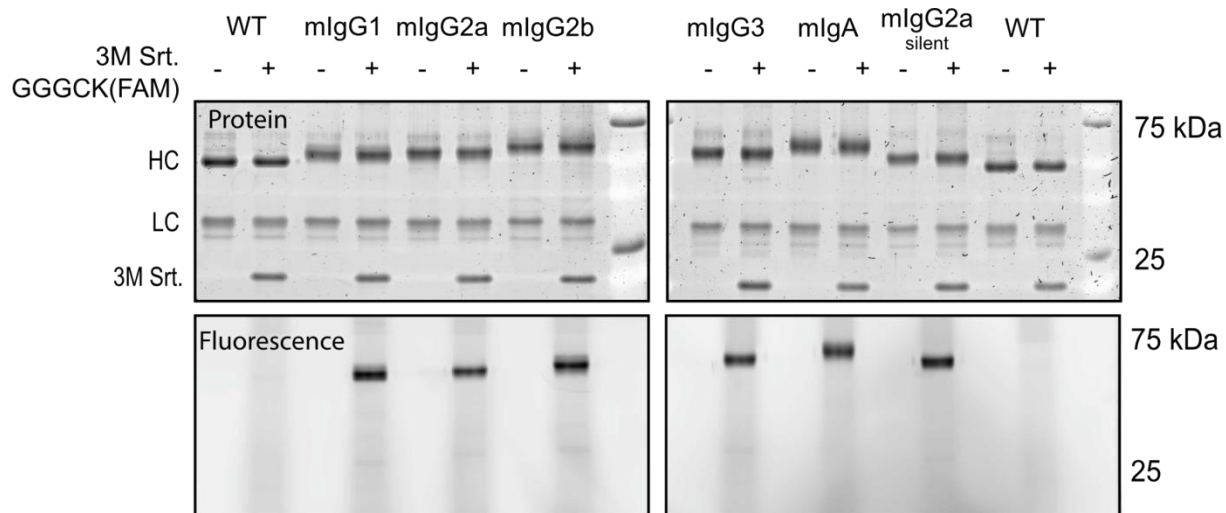


Fig. S4. Raw images of sortagging of MIH5 isotype variants. Raw images of protein and fluorescent SDS-page scans of sortagging of MIH5 isotype variants as displayed in Fig. 2E. Of each antibody 5 μ g was incubated with 1 molar equivalent of 3m Sortase (3m Srt) and 100 molar equivalent GGGCK(FAM) for one hour. From each reaction 500ng was run on reducing SDS-PAGE. Subsequently, protein and fluorescent images of the SDS-page were acquired.

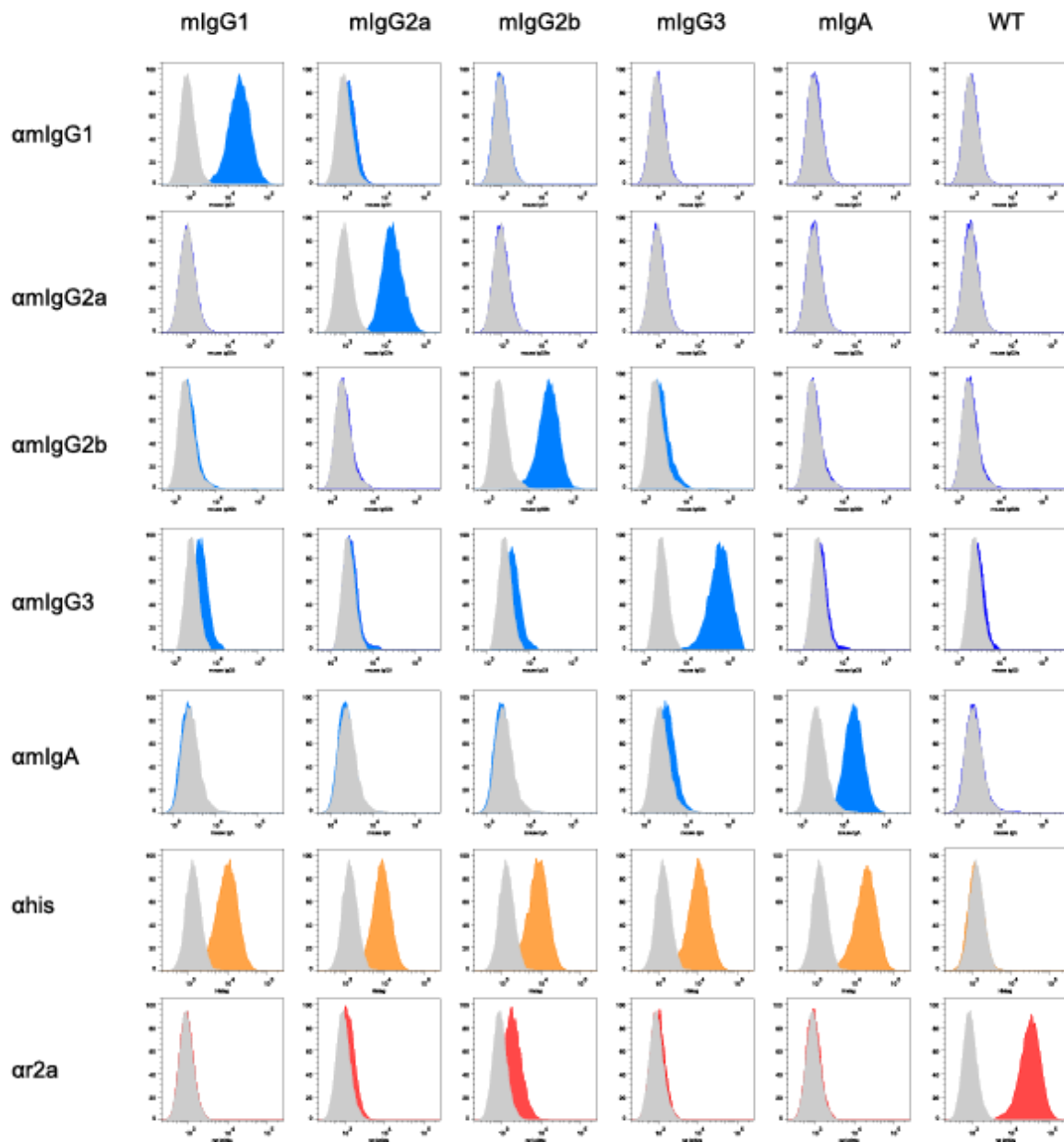


Fig. S5. Murine isotype panel generation of NLDC-145 via CRISPR/HDR. The CRISPR/HDR strategy as outlined in Fig. 2 was applied to the NLDC-145 to obtain recombinant hybridomas secreting murine IgG1, IgG2a, IgG2b, IgG3 and IgA. For each isotype, hybridoma supernatant was used to stain DEC205 expressing cell line JAWS II in combination with a panel of secondary antibodies against rat IgG2a, his-tag and murine isotypes.

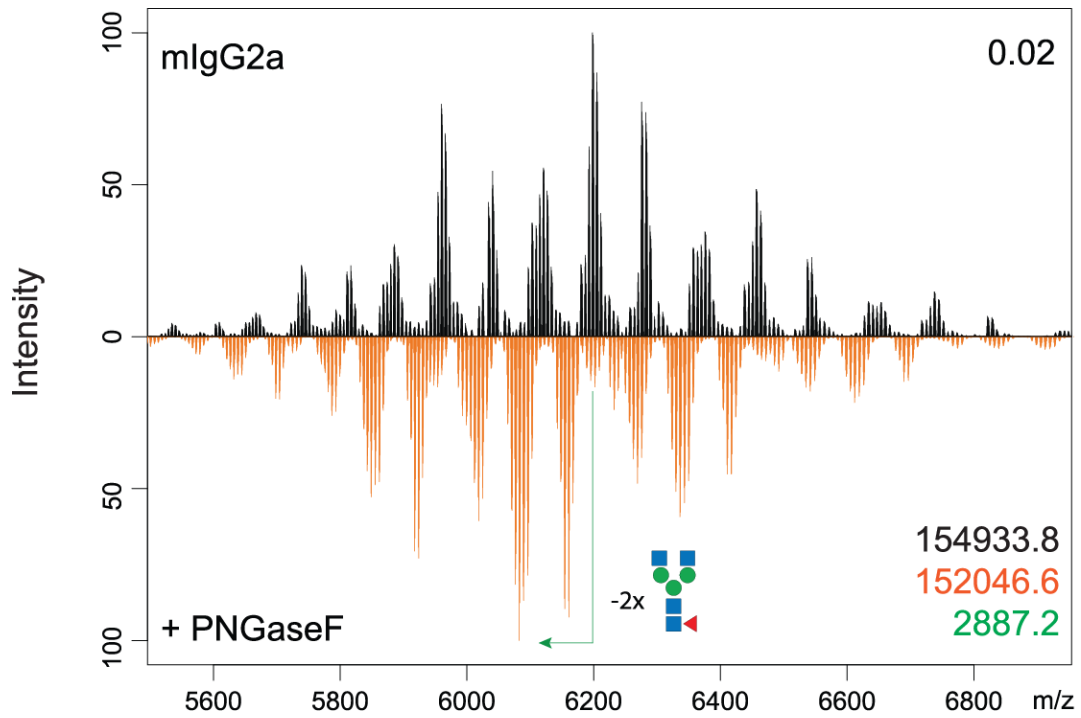
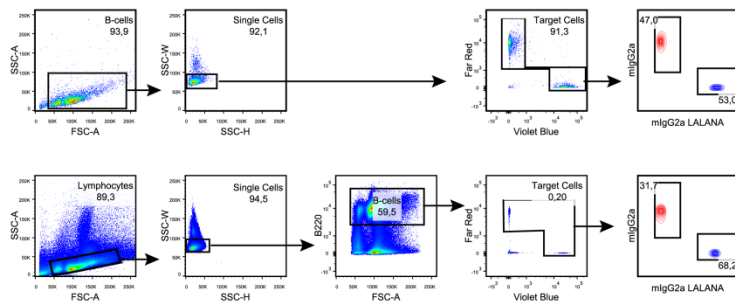


Fig. S6. Glycosylation profile of MIH5 mIgG2a via native mass spectrometry. Purified MIH5 mIgG2a was treated overnight with PNGaseF (orange) and compared to an untreated sample (black) via high resolution native mass spectrometry. The Pearson correlation coefficient between the two spectra over all ion signals is given in the upper right corner. The molecular mass belonging to the base peak of the untreated (black font) and treated (orange font) sample and the leading difference in mass (green) is depicted in the lower right corner. The difference in mass between treated and untreated samples indicates the loss of two glycans.

A Gating Strategy



B

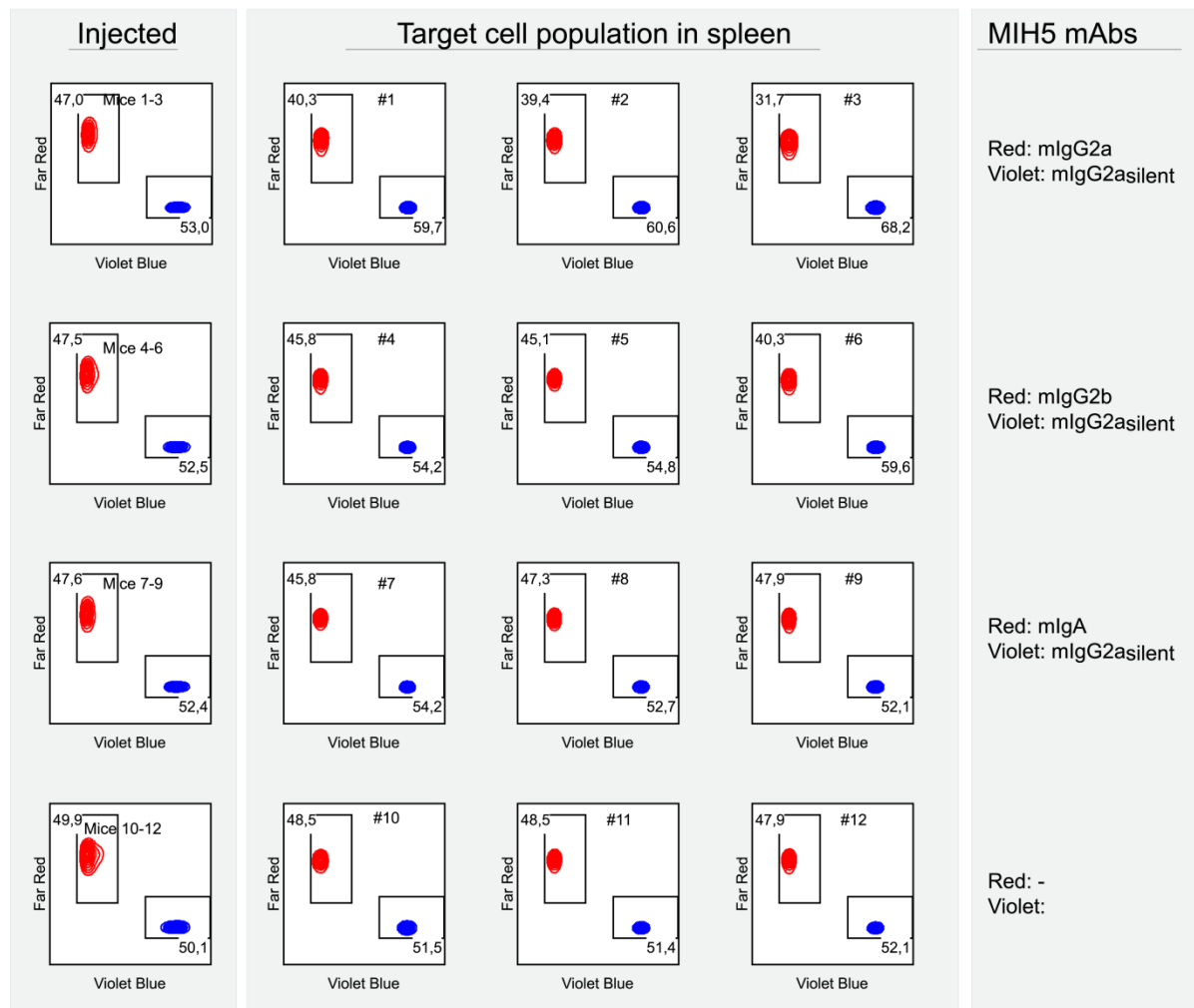


Fig. S7. Gating and FACS plots of isotype-dependent depletion in vivo. Isolated B-cells were stimulated overnight with IFN- γ and labeled with either red or violet tracer dyes. Subsequently, the violet B-cells were opsonized with MIH5 mIgG2a_{silent}, while the red B-cells were opsonized with MIH5 mIgG2a, mIgG2b or mIgA. The populations were mixed and intravenously injected into LPS stimulated BL/6 mice. After 24 hours the mice were sacrificed and spleens isolated to determine the

ratio of violet blue and far red target cells. These were used to determine the isotype dependent target cell depletion. The gating strategy (**A**) and the plots (**B**) depicting the labeled B-cell ratios used for determining the specific target depletion in Fig 5C are given.

Table S1. Fab' donor construct for HDR. Table displays sequences of each feature of the donor construct used to convert rat IgG2a hybridomas to sortagable Fab' fragment secreting cell lines.

| Isotype | Sequence |
|----------------------------------|--|
| 5' HA | CCTGGAACCTCTGGAGCCCTGTCCAGCGGTGTGCACACCTTCCCAGCTGTCTGCAGTCTGGACTCTACACTCTCACCAGCTCAGTGACTGTACCCTCCAGCACCTGGTCCAGCCAGGCCGTACCTGCAACGTAGCCACCCGGCCAGCAGCACCAAGGTGGACAA GAAAATTGGTGAGAGAACAACCAGGGGATGAGGGGCTACTAGAGGTGAGGATAAGGCATTAGATTGCCTACACCAACCAGGG TGGGCAGACATCACCAGGGAGGGGGCCTCAGCCCAGGAGACCAAAAATTCTCCTTTGTCTCCCTTCTGGAGATTTCTATGTCCT TTACACCCATTTATTAATATTCTGGGTAAGATGCCCTTGATCATGACATACAGAGGCAGACTAGAGTATCAACCTGCAAAAGGTC ATACCCAGGAAGAGCCTGCCATGATCCACACCAGAACCAACCTGGGGCCTTCTCACCTATAGACCATACTAACACACAGCCTT CTCTCTGCAGTGCCAAAG |
| Sortag, his-tag, Stop | GGAAGGAGGGCGGAGGCAGCCTGCCGAAACCGGCGGCCATCATCATCATCATTGA |
| IRES | GGATCCCAATTGCTCGAGGCCCTCTCCCTCCCCCCCCCTAACGTTACTGGCCGAAGCCGCTTGGAAATAAGGCCGGTGTGCG TTTGTCTATATGTTATTTCCACCATATTGCCGTCTTTTGGCAATGTGAGGGCCCGAAACCTGGCCCTGTCTTCTTGACGAGCAT TCCTAGGGGTCTTTCCCTCTCGCCAAAGGAATGCAAGGTCTGTTGAATGTCGTGAAGGAAGCAGTTCCTCTGGAAGCTTCTTG AAGACAAACAACGTCTGTAGCGACCCCTTTCAGGCAGCGGAACCCCCACCTGGCGACAGGTGCCTCTGCGGCCAAAAGCCAC GTGTATAAGATACACCTGCAAAAGCGGCCACAACCCCAAGTCCACGTTGTGAGTTGGATAGTTGTGAAAGAGTCAAATGGCTCT CCTCAAGCGTATTCAACAGGGGCTGAAGGATGCCAGAAGTACCCATTGTATGGGATCTGATCTGGGGCCTCGGTGCACA TGCTTTACATGTGTTTAGTCGAGGTTAAAAAACGTCAGGCCCCCGAAACCAGGGGACGTGGTTTTCTTTGAAAAACACGAT GATAATATGGCCACAGAATTCGCCACC |
| <i>Bsr</i> | TGGCCAAGCCTTTGTCTCAAGAAGAATCCACCCTCATTGAAAGAGCAACGGCTACAATCAACAGCATCCCCATCTCTGAAGACTA CAGCGTCCAGCGCAGCTCTCTCTAGCGACGCCGCATCTTCACTGGTGTCAATGTATATCATTCTTACTGGGGACCTTGTGC AGAACTCGTGGTCTGGGCACTGCTGCTGCTGCGGCAGCTGGCAACCTGACTTGTATCGTCGCGATCGGAAATGAGAACAGGG GCATCTTGAGCCCTGCGGACGGTGCAGAGGTGCTTCTCGATCTGCATCCTGGGATCAAAGCCATAGTGAAGGACAGTGAT GGACAGCCGACGGCAGTTGGGATTCGTGAATTGCTGCCCTCTGTTATGTGTGGGAGGGCTAAGTACTAGTCGA |
| SV40 polyA terminati on | GTAAGTACTGACTGTGCCTTCTAGTTGCCAGCCATCTGTTGTTTGGCCCTCCCCCGTGCCTTCTTACCCTGGAAGGTGCCAC TCCCCTGTCTTTTCTAATAAAATGAGGAAATTGCATCGCATTGTCTGAGTAGGTGTCATTCTATTCTGGGGGGTGGGGTGGGG CAGGACAGCAAGGGGGAGGATTGGGAAGACAATAGCAGGCATGCTGGGATGCGGTGGGCTCTATGGAGATCTTTGACA |
| 3'HA | GGTAAGTCACTAGGACTATTACTCCAGCCCCAGATTCAAAAAATATCCTCAGAGGCCATGTTAGAGGATGACACAGCTATTGAC CTATTTCTACCTTTCTTCTTCTACAGGCTCAGAAGTATCATCTGTCTTCTATCTTCCCCCAAGACCAAAGATGTGCTCACCAT CACTCTGACTCCTAAGGTCACGTGTGTTGTGGTAGACATTAGCCAGAATGATCCCGAGGTCCGGTTCAGCTGGTTTATAGATGA CGTGGAAGTCCACACAGCTCAGACTCATGCCCGGAGAAAGCAGTCCAACAGCACTTTACGCTCAGTCAGTGAACCTCCCCATCGT GCACCGGGACTGGCTCAATGGCAAGACGTTCAAATGCAAAAGTCAACAGTGGAGCATTCCCTGCCCCCATCGAGAAAAGCATCTC CAAACCCGAAGGTGGGAGCAGCAGGGTGTGTGGTGTAGAAGCTGCAGTAGGCCATAGACAGAGCTTGACTTAACTAGACTT |

Table S3. FcγR affinity values of MIH5 Fc variants and comparison to literature. Affinity quantification by K_D (μM) of CRISPR/HDR antibodies for mFcγRI, FcγRIIb and mFcγRIV (**bold**) comparison to described values in literature.

| Fc variant | mFcγRI | mFcγRIIb | mFcγRIV |
|--------------------------------|---|---|---|
| mIgG1 | -/- -/- (28–32) | 0.26 ± 0.05 0.15 (28); 0.30 (32); 0.83 (29); 0.17 (30); | -/- -/- (28–32) |
| mIgG2a | 0.017 ± 0.007 0.012 (28); 0.006 (32) 0.026 (29); 0.018 (30); 0.033 (31); 0.013 - 0.022 (33) | 0.66 ± 0.20 0.69 (28); 2.4 (32); 1.8 (29) | 0.13 ± 0.02 0.060(28); 0.035(32); 0.071(29); 0.010(30) |
| mIgG2b | -/- -/- (28, 29, 33); 0.021 (33) | 1.24 ± 0.06 0.83 (28); 0.45 (32); 0.91 (29); | 0.20 ± 0.02 0.12 (28); 0.059 (32); 0.063 (29); |
| mIgA | -/- -/- (31) | -/- -/- (31) | -/- -/- (31) |
| mIgG2a_{silent} | -/- -/- (26) | -/- -/- (26) | -/- -/- (26) |